J. Membrane Biol. 214, 139–146 (2006)
DOI: 10.1007/s00232-006-0056-8

The Journal of
Membrane
Biology



# Association of Renal Na,K-ATPase α-Subunit with the β- and γ-Subunits Based on Cryoelectron Microscopy

**P. Purhonen**[1,2], **K. Thomsen**[3], **A.B. Maunsbach**[3], **H. Hebert**[1]

[1]Karolinska Institutet, Department of Biosciences and Nutrition and School of Technology and Health, Royal Institute of Technology, S-141 57 Huddinge, Sweden

[2]Institute of Medical Technology, University of Tampere, FI-33014, Tampere, Finland

[3]Water and Salt Research Center, Department of Cell Biology, Institute of Anatomy, University of Aarhus, DK-8000, Aarhus, Denmark

Received: 10 July 2006/Revised: 29 November 2006

**Abstract.** Na,K-ATPase transports $Na^+$ and $K^+$ across cell membranes and consists of α- and β-subunits. Na,K-ATPase also associates with small FXYD proteins that regulate the activity of the pump. We have used cryoelectron microscopy of two-dimensional crystals including data to 8 Å resolution to determine the three-dimensional (3-D) structure of renal Na,K-ATPase containing FXYD2, the γ-subunit. A homology model for the α-subunit was calculated from a $Ca^{2+}$-ATPase structure and used to locate the additional β- and γ-subunits present in the 3-D map of Na,K-ATPase. Based on the 3-D map, the β-subunit is located close to transmembrane helices M8 and M10 and the γ-subunit is adjacent to helices M2 and M9 of the α-subunit.

**Key words:** Na,K-ATPase — Cryoelectron microscopy — γ-subunit — β-subunit — FXYD2

## Introduction

Na,K-ATPase establishes the differences in $Na^+$ and $K^+$ concentrations across the plasma membrane by pumping three $Na^+$ ions out of and two $K^+$ ions into the cells, maintains the osmotic balance of cells and drives $Na^+$-coupled secondary transport of various substances. Na,K-ATPase is an oligomer composed of α- and β-subunits. The catalytic α-subunit (~112 kDa) has 10 putative transmembrane (TM) α-helices and three cytoplasmic domains: the nucleotide binding (N), phosphorylation (P) and actuator (A) domains, as in the related $Ca^{2+}$-ATPase of the sarcoendoplasmic reticulum (SERCA) (Toyoshima et al., 2000). The β-subunit protein (~35 kDa) has one TM span and an extracellular part containing three conserved glycosylation sites. The β-subunit is needed for correct membrane insertion and folding of the α-subunit but also affects the ion affinities of the pump (Geering, 2001). In addition, Na,K-ATPase associates in a tissue-specific manner with members of the *FXYD* gene family of small ion transport regulators (Sweadner & Rael, 2000). The first FXYD protein to be identified was the γ-subunit (Forbush, Kaplan & Hoffman, 1978) (~7kDa), which shifts the conformational equilibrium of the pump toward E1 but also increases the $K^+$ antagonism of $Na^+$ activation (Therien et al., 2001). Five other FXYD family members, most recently FXYD5 (RIC, related to ion channel) (Lubarski et al., 2005), have been found to interact with Na,K-ATPase and to regulate its activity.

The model of the Na,K-ATPase reaction cycle, known as the Albers-Post scheme, describes how ion binding, occlusion and release to the opposite side of the membrane are coupled to pump phosphorylation by ATP and conformational transition between the E1 and E2 states (Jørgensen, Håkansson & Karlish, 2003). E1 binding sites face the cytoplasm and have high affinity for $Na^+$, whereas E2 sites are oriented toward the extracellular space and have higher affinity for $K^+$. Dephosphorylation of the pump from E2-P[2K] leads to the occluded state E2[2K].

Na,K-ATPase belongs to a large family of P-type ATPases (Axelsen & Palmgren, 1998), which are characterized by the formation of a transient covalently bound aspartylphosphate intermediate during the reaction cycle. Structurally, the best-characterized member of the P-type ATPases is SERCA, for which the atomic structure is now known in E1 (Toyoshima et al., 2000), E2 (Toyoshima & Nomura, 2002; Obara

*Correspondence to:* H. Hebert; email: Hans.Hebert@csb.ki.se

et al., 2005) and various phosphorylated forms (Sørensen, Møller & Nissen, 2004; Toyoshima & Mizutani, 2004; Toyoshima, Nomura & Tsuda, 2004; Olesen et al., 2004; Jensen et al., 2006). The atomic structures in different conformations have helped us to understand the transport cycle of $Ca^{2+}$ at the molecular level and have shown large movements of the cytoplasmic domains and rearrangements of the TM α-helices during the enzymatic cycle. In contrast to Na,K-ATPase, SERCA has no β- or γ-subunit.

We have previously determined the three-dimensional (3-D) structure of Na,K-ATPase from pig kidney at 9.5 Å resolution in the membrane plane using electron crystallography (Hebert et al., 2001). The Na,K-ATPase 3-D structure from supraorbital glands of salt-adapted ducks was reported at 11 Å resolution (Rice et al., 2001). Both 3-D structures showed the cytoplasmic domains divided into three distinct domains as in $Ca^{2+}$-ATPase (Toyoshima et al., 2000), as well as extra densities, probably arising from the β- (Hebert et al., 2001; Rice et al., 2001) and γ- (Hebert et al., 2001) subunits. We have now improved the 3-D map of renal Na,K-ATPase by collecting more data from 2-D crystals, by reprocessing all images and by including data to 8 Å resolution. A homology model for the α-subunit was constructed based on a $Ca^{2+}$-ATPase structure (Toyoshima & Nomura, 2002). Docking to the 3-D map showed the location of the β-subunit close to helices M8 and M10 and that of the γ-subunit adjacent to the groove formed by helices M2, M4, M6 and M9.

## Materials and Methods

### Enzyme Purification and 2-D crystallization

Na,K-ATPase was isolated in membrane-bound form from the outer medulla of pig kidney as a microsomal fraction and purified by isopycnic zonal centrifugation in the presence of ATP and sodium dodecyl sulfate (Jørgensen, 1988). The membrane fragments were dialyzed at +4°C for 1 day against 10 mM imidazole-HCl (pH 7.3) in a buffer containing 1 mM $NH_4VO_3$, 5 mM $MgCl_2$, 5 mM $CaCl_2$ and 0.3 mM phospholipase $A_2$ to produce 2-D crystalline arrays of Na,K-ATPase.

### Cryoelectron Microscopy and Image Processing

Samples of 2-D crystalline membranes, 2–2.5 μl, on carbon-coated electron microscopic grids were blotted and plunge-frozen into ethane with either a Reichert-Jung KF80 cryofixation unit, a Leica EM-CPC (Leica Microsystems, Wetzlar, Germany) or a Vitrobot™ (FEI Company, Eindhoven, The Netherlands). Frozen samples were stored under nitrogen and transferred to an electron microscope using a Gatan cryoholder (model 626). Data were collected under low-dose conditions on Kodak (Rochester, NY) SO-163 electron micrograph films with Philips CM120, Tecnai F12 (FEI Company) and JEOL JEM-2100F (JEOL, Tokyo, Japan) electron microscopes. A nominal magnification of 50,000 and defocus of 0.5–2.5 μm were used. The best crystalline areas were selected with optical diffractometry and digitized with a Zeiss (Oberkochen, Germany) Scai scanner operated at a pixel size of 7 μm. Images were processed with the MRC program suite (Crowther, Henderson & Smith, 1996). For reprocessing, the MAKETRAN program (Kunji et al., 2000) was used with a generated 3-D map of Na,K-ATPase from 151 images as a reference for crystal unbending. Images were corrected for contrast transfer functions by the programs CTFFIND and TTREFINE. The 3-D map was calculated with CCP4 programs (CCP4, 1994) and visualized in O (Jones et al., 1991). The point-spread function was calculated by setting the amplitudes and phases in the data set to 1 and 0, respectively.

### Homology Modeling and Docking

Sequence alignment of the Na,K-ATPase $\alpha_1$-subunit (Swiss-Prot accession P05024) and SERCA 1a was done with MODELLER (Šali & Blundell, 1993) version 8v1 with manual corrections and utilizing information from previous alignments (Sweadner & Donnet, 2001; Kühlbrandt, 2004; Keenan et al., 2005). The alignment of the N domain was done mainly according to the determined nuclear magnetic resonance (NMR) structure of rat $\alpha_1$ (Hilge et al., 2003). The N-terminal Na,K-ATPase sequence before the alignment starting point (methionine 39) was cut off before modeling. One hundred homology models were constructed with MODELLER using the 3.1 Å resolution $Ca^{2+}$-ATPase structure 1IWO (Toyoshima & Nomura, 2002) as a template. The selected model showed the lowest value of the MODELLER objective function. TM segments for porcine β- and γ-subunits, composed of residues W32-I61 for β (P05027) and R26-S46 for γ (Füzesi et al., 2005), were generated in O and placed manually to the densities of the 3-D map. The homology model was docked to the map using Situs (Wriggers, Milligan & McCammon, 1999). Structures were visualized in PyMOL (http://pymol.sourceforge.net) and Chimera (Pettersen et al., 2004).

## Results and Discussion

### Sequence Alignment and Homology Model

Alignment of the pig Na,K-ATPase $\alpha_1$-subunit with SERCA (Fig. 1) was started from methionine 39 as in Kühlbrandt (2004) and Keenan et al. (2005). Except for the N and P domains, only short gaps were needed to align the two sequences, and their positions corresponded relatively well to previous alignments (Sweadner & Donnet, 2001; Kühlbrandt, 2004; Keenan et al., 2005).

The 2-D crystals were prepared in the presence of orthovanadate, which stabilizes the protein in a conformation resembling a transition state of E2-P hydrolysis (Cantley, Cantley & Josephson, 1978). A similar transition state analogue is obtained with $AlF_4^-$, and a homology model was first built from the $Ca^{2+}$-ATPase structure with bound $AlF_4^-$ (Olesen et al., 2004) (*data not shown*). However, a slightly better match between the cytoplasmic domains in the 3-D map and the model was obtained when the SERCA structure in the E2 state (Toyoshima & Nomura, 2002) was used as a template for the homology model (Fig. 2). The cytoplasmic domains

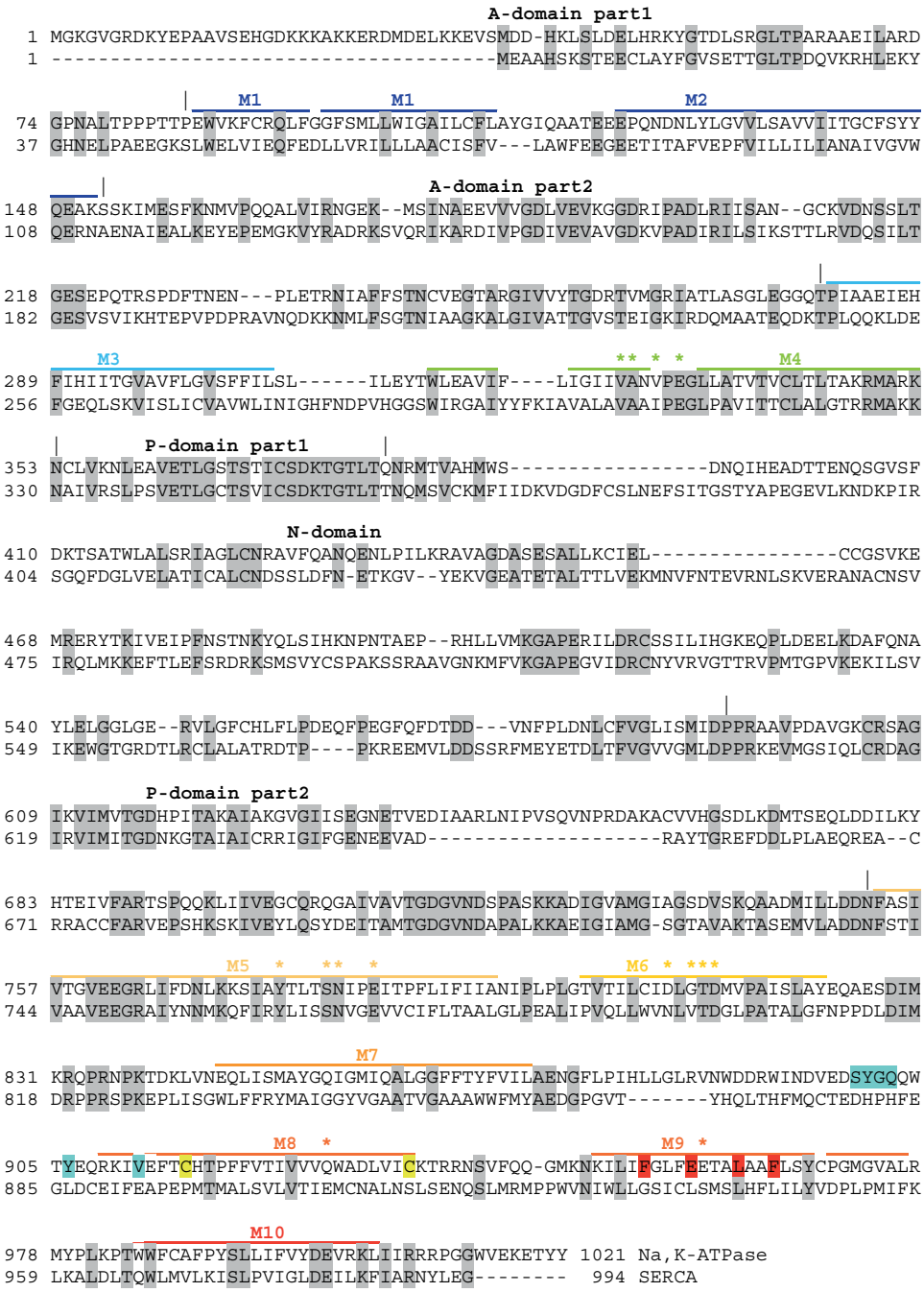


**Fig. 1.** Sequence alignment of the pig $\alpha_1$-subunit of Na,K-ATPase (*upper sequence*) with SERCA1a. Identical residues in the alignment are shown with gray boxes. Proposed TM helical segments from the Na,K-ATPase model are marked with colored lines. Residues of loop L7/8 making contact with the β-subunit are colored cyan and cysteine residues C916 and C935 of M8, yellow. Residues F954, E958, L962 and F965 of helix M9, proposed to present the contact surface for FXYD proteins (Li et al., 2004), are colored red. Stars show the residues coordinating ion binding (Ogawa & Toyoshima, 2002). Residues for the Na,K-ATPase sequence are numbered according to the pig enzyme.

might show small differences in their spatial organization between these two ATPases or between the vanadate and $AlF_4^-$ transition states. Some differences of the domain structures are expected as noticeable sequence variations occur at the N and at part of the P domains (Fig. 1). The 3-D structure of the Na,K-ATPase N domain has been determined with NMR (Hilge et al., 2003) and X-ray crystallography (Håkansson, 2003) and has the same overall fold as the N domain of SERCA, with structural differences mainly found at the areas of large inserts (Hilge et al., 2003; Håkansson, 2003). Considering the obtained resolution of the present 3-D map, the N domain was modeled based on the $Ca^{2+}$-ATPase structure (Toyoshima & Nomura, 2002) in order to keep the cytoplasmic domains in one known conformation relative to each other.

In comparison with the E2 structure of SERCA (Toyoshima & Nomura, 2002), the Na,K-ATPase model suggests some changes in the N-terminal TM helices, most noticeably with a longer M2 helix and a more unwound M4 structure than in $Ca^{2+}$-ATPase; but the lengths and positions of M3-M6 are very similar to SERCA. This is in accordance with the

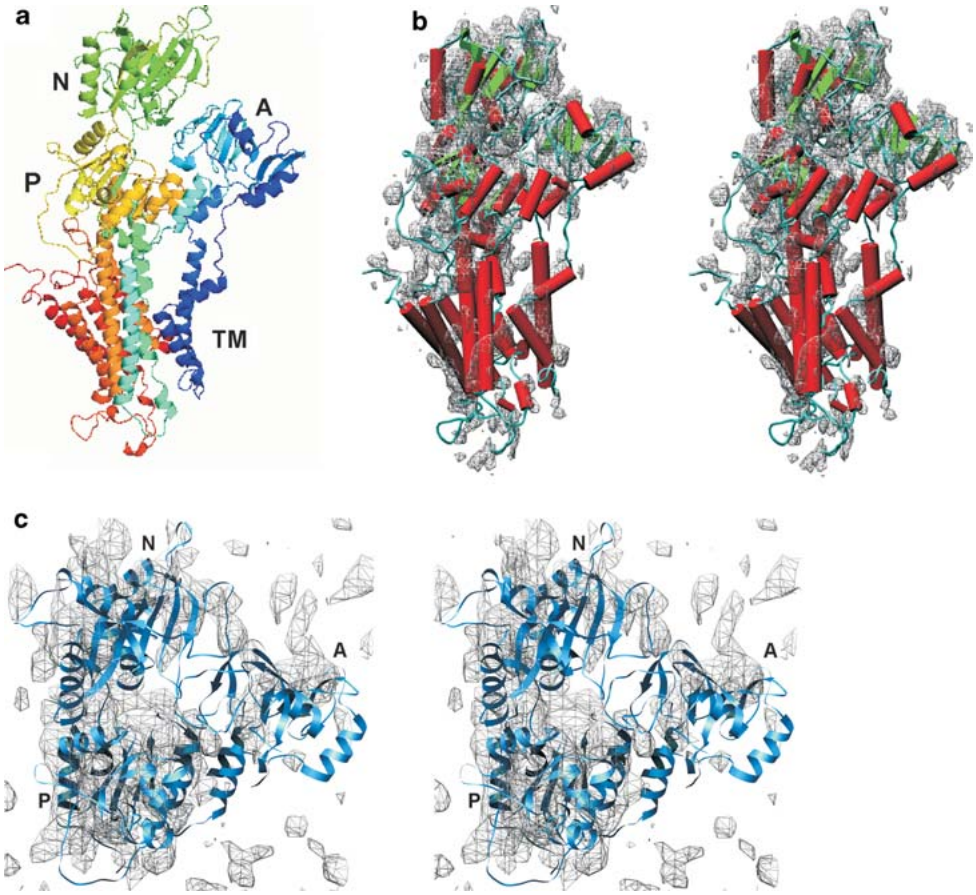


**Fig. 2.** (*a*) A ribbon representation of the Na,K-ATPase α-subunit homology model based on the SERCA E2 structure (Toyoshima & Nomura, 2002). Colors change from amino (blue) to carboxy (red) terminus. The cytoplasmic N, P and A domains and the TM area are indicated. (*b*) Homology model docked to the 3-D map in stereo view. The map was masked around the homology model. (*c*) A slice in stereo through the 3-D map at the height of the cytoplasmic domains showing correspondence between the model and the 3-D map. The approximate thickness is 75 Å.

more conserved nature of M4-M6 and their proposed central role in ion binding. The suggested ion-binding sites are organized similarly to the model proposed by Ogawa & Toyoshima (2002). The C-terminal helices M7-M9 show slight shifts in their helical positions in comparison to SERCA.

## 3-D Structure

The present 3-D map was constructed from 145 2-D crystalline areas, which contained the α-, β- and γ-subunits, as previously shown (Hebert et al., 2001). In image processing, the amount of defocus was carefully determined and the inherent translational disorder corrected for by unbending the crystals (Kunji et al., 2000) against a low-resolution Na,K-ATPase 3-D map. This improved the information content of individual images and increased the number of observations along the Fourier transform lattice lines. The new 3-D map was calculated using data to 8 Å resolution (Table 1) and an estimated vertical resolution of 15 Å. The phases show better statistics in the hk0 plane (calculated as deviations from 0° or 180°) compared to the complete merged data set (Table 1). This may be related to the limitation of conventional crystallographic processing to correct only for in-plane lattice distortions. The improvement of the 3-D map was most clearly seen from the cytoplasmic domains (Fig. 2), which were defined better than in the previous 3-D map (Hebert et al., 2001). As previously, clear density peaks were observed in sections drawn through the TM area, but in the 3-D map these did not form continuous densities to allow independent mapping of the TM α-helices. The expected tilts of some of the TM helices as reported for SERCA (Toyoshima et al., 2000; Toyoshima & Nomura, 2002), and their flexibility in the 2-D crystals might contribute to their weaker appearance in the 3-D map.

## The β- and γ-Subunits

The high degree of similarity between our map and the $Ca^{2+}$-ATPase structure on the cytoplasmic side was used to align the map and the Na,K-ATPase homology model manually. The initial manual alignment was verified by automatic docking using Situs (Wriggers et al., 1999), causing only minor changes. Additional densities in the TM domain of the Na,K-ATPase 3-D map not covered by the α-subunit homology model were used to locate the β- and γ-subunits (Fig. 3). One of the densities is located in the groove between adjacent α-subunits in the 2-D crystals and is near the crystallographic twofold axis.

**Table 1.** Crystallographic data

| | |
|---|---|
| Space group symmetry | P2 |
| Unit cell parameters | α = 146.5 Å, β = 51.6 Å, γ = 96.5 Å |
| Phase deviation from 0° or 180° (deg.) | 200–14 Å (22.1) |
| | 14–10 Å (31.4) |
| | 10–8 Å (35.9) |
| | Overall 24.3 |
| Number of crystalline areas[a] | 145 |
| Resolution limit for merging (Å) | 8.0 |
| Vertical resolution[b] | 15.0 |
| Number of amplitudes and phases (IQ 1–7) | 12,445 |
| Phase residual[c] (deg.) | 200–14 Å 30.0 (371) |
| | 14–10 Å 47.7 (516) |
| | 10–8.1 Å 57.2 (501) |
| Merged overall phase residual[d] (deg.) | 41.8 |
| Weighted merging R factor (%) | 43.8 |

[a]Distribution of tilt angles: 0–10°, 14 images; 10–20°, 16; 20–30°, 35; 30–40°, 45; 40–50°, 28; 50–61°, 7.
[b]Estimated from point-spread function.
[c]From merging image data (IQ 1–4), random value 90. Number of spots in parentheses.
[d]From lattice line adaptation.

It is positioned close to helices M8 and M10, with a continuation from the membrane area toward the extracellular space, and is identified as the β-subunit. Analysis of tubular crystals from supraorbital glands (Rice et al., 2001) suggested the TM location for the β-subunit to be near M7 and M10, based on the extra density observed at the cytoplasmic and extracellular membrane surfaces. The same position was proposed in a work using thermal denaturation (Donnet, Arystarkhova & Sweadner, 2001). However, in our 3-D map a density was found in the TM area near M8 (Fig. 3). In addition, a close distance to M10 near the extracellular side was observed and M7 lies behind M10. Location of the TM helix of β close to M8 would be compatible with the suggested chemical cross-link between cysteine C45 of β and either C916 or C935 of M8 in detergent-solubilized samples (Or, Goldshleger & Karlish, 1999; Ivanov, Modyanov & Askari, 2000). The known contacts between β and the α-subunit loop L7/8 at the extracellular side (Colonna, Huynh & Fambrough, 1997; Wang & Farley, 1998) seem also possible from this site, considering the tilt of the βTM helix (Fig. 4a). The conserved tyrosines Y39 and Y43 of the β-subunit, shown to be important for transport kinetics of Na,K-ATPase (Hasler et al., 2001), would be oriented toward M10 from this position (Fig. 4a). At the other side of the helix of β, the putative helix dimerization motif GXXXGXXXG (Hasler et al., 2001) is positioned favorably for association with another β-subunit in the 2-D crystals. The exact residues responsible for the contact remain unclear as also C45 of β near the glycines has been indicated as a site for β-β association (Ivanov, Zhao & Modyanov, 2002). Participation of C45 in the β-β contacts might require a slight rotation of the β TM helix from that shown in Figure 4a. The C-terminal sequence after M10 could also participate in crystal contacts between two adjacent α-subunits in these 2-D crystals.

Another strong additional density in the 3-D map was found close to helices M9 and M2 and was assigned to the γ-subunit (Fig. 3). Our previous 3-D structure suggested a position of γ close to M9 and M2 (Hebert et al., 2001), and a location between M9 and M10 has also been proposed (Donnet et al., 2001). Later mutational analysis has shown that F954, E958, L962 and F965 of M9 would form one contact surface with FXYD proteins (Li et al., 2004). Further support for the location of γ in the groove of M9, M6, M4 and M2 came from cross-linking studies of the cytoplasmic part of the γ-subunit and modeling of the α-γ interactions (Füzesi et al., 2005). The present 3-D map shows a position of γ close to M9 and M2 at the TM domain. At the cytoplasmic side, γ becomes close to the stalk region of M4, supporting possible cross-link to K347 (Füzesi et al., 2005); but the path for the rest of the cytoplasmic tail, which might have an unordered structure, cannot be followed in the 3-D map. The 3-D map reveals a slight tilt for γ relative to the normal of the membrane plane and in relation to M9 (Fig. 4a). Previously, solid-state NMR (Franzin et al., 2004) has suggested low tilt angles for the TM helices of FXYD proteins.

FXYD proteins have conserved residues in the TM part, which are mainly clustered to one side of the helical wheel (Sweadner & Rael, 2000) and are supposed to be important for the interactions with the α-subunit. The strongest density in the 3-D map is located outside of the actual groove between M9 and M2, where the conserved face is oriented toward the groove (Fig. 4a). Based on the 3-D map and the homology model, the γ-subunit is close to M9 residues L962 and F965 (Fig. 4b), suggested to contribute to the stability of the α-γ association (Li

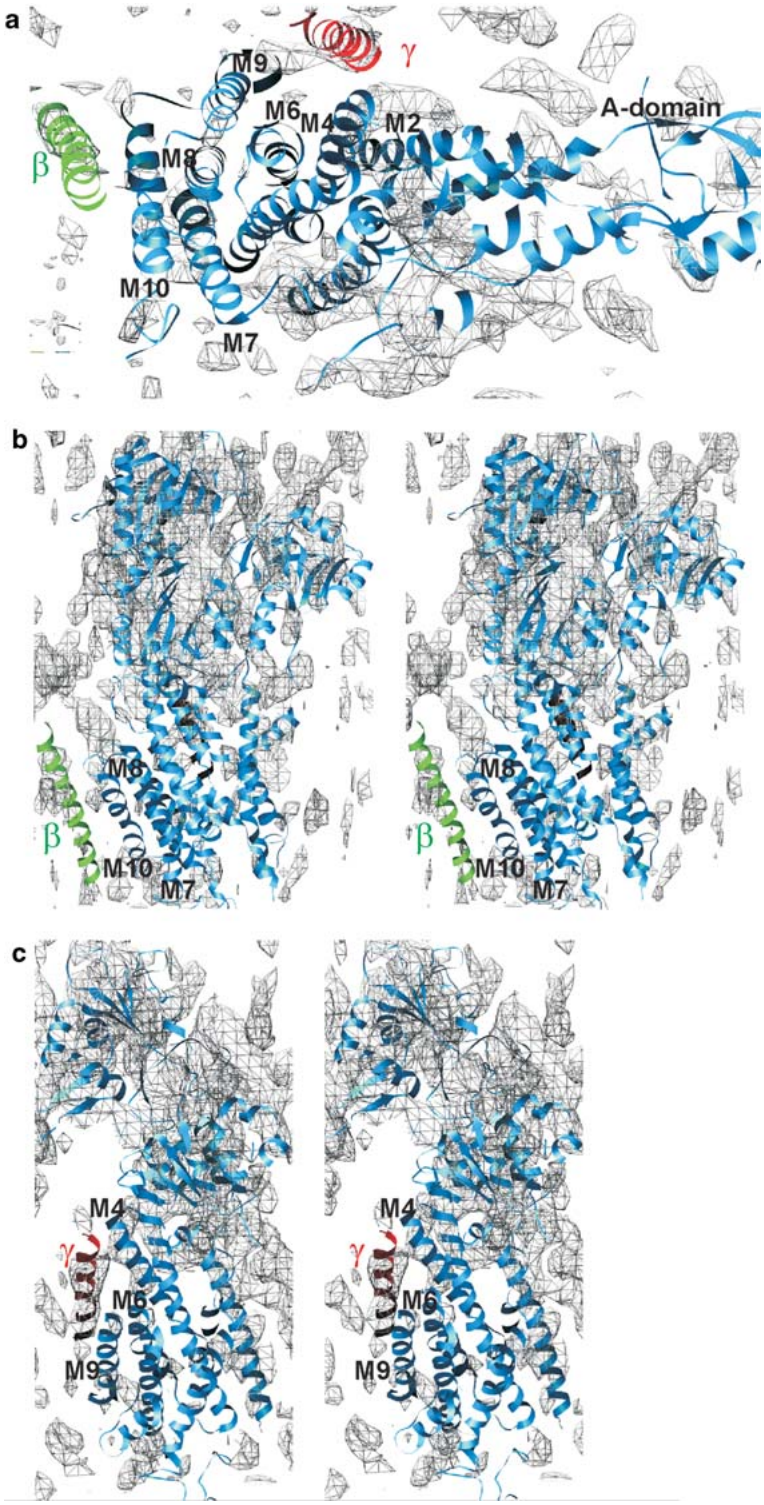


**Fig. 3.** Docking the homology model to the 3-D map revealed additional densities that were used to localize the β- and γ-subunits. (*a*) A view from the cytoplasm toward the TM area. Stereo views showing (*b*) the β- and (*c*) the γ-subunits in association with the α-subunit.

et al., 2004). The γ-subunit is also close to M814 and V815 in M6 (Fig. 4b). By interacting with residues in M6 and M9, the γ-subunit might cause local changes in the TM helices that could slightly modify the nearby ion-binding site (Ogawa & Toyoshima, 2002) and change ion affinities. Although the functional effects of γ to ion affinities are thought to be mediated by the TM domain (Pu, Scanzano & Blostein, 2002), the complex interplay between α and γ (Füzesi et al., 2005) creates other possibilities. In fact, the extracellular loop L7/8 of the α-subunit was recently pointed out as a potent modulator in $K^+/Na^+$ antagonism (Zouzoulas & Blostein, 2006).

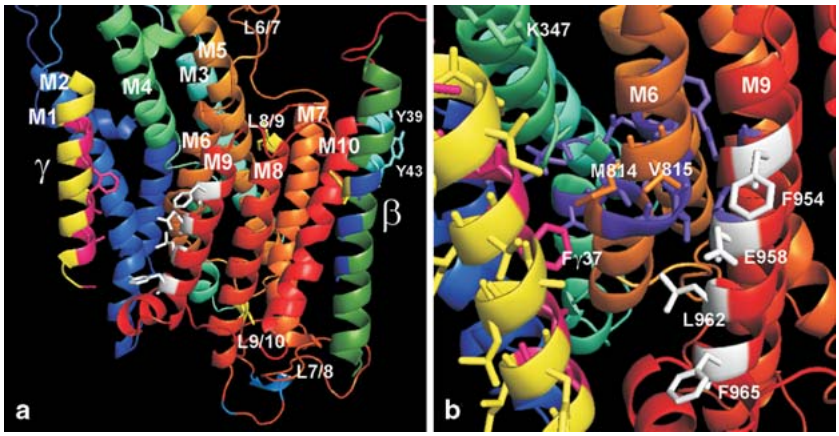


**Fig. 4.** (*a*) The TM area and extracellular loops of the Na,K-ATPase homology model visualized in PyMOL. The view is slightly tilted relative to the membrane plane to show the extracellular contact sites between the α- and β-subunits in loop L7/8 (Colonna et al., 1997; Wang et al., 1998) (marine blue). The positions of the subunits are those defined in Figure 2. Helices and visible loops are marked with numbers. Cysteine residues C916 and C935 of M8 and C45 of the β are colored yellow. The residues of helix M9 forming the contact surface for FXYD proteins (Li et al., 2004) are white. Also marked are tyrosines Y39 and Y43 (cyan), glycine residues of the dimerization motif (Hasler et al., 2001) (dark blue) in the β-subunit as well as the conserved residues of FXYD proteins in the TM helix of the γ-subunit (pink). Only the suggested TM helical segments are shown for β and γ. (*b*) A closer view of the γ-subunit (yellow) and M9 with some residues marked. The suggested ion-binding residues in the α-subunit are colored purple.

At present, it is unknown whether γ remains associated with Na,K-ATPase throughout the enzymatic cycle or if smaller changes in relation to the α-subunit occur during the conformational changes. Interestingly, in SERCA, the same groove is suggested to be the binding site in the E2 conformation for the inhibitor phospholamban (Toyoshima et al., 2003). $Ca^{2+}$ binding in E1 conformation narrows this groove by moving M2 toward M9 and leads to the dissociation of phospholamban (Toyoshima et al., 2003). Within the membrane plane the closest γ-α and β-α backbone distances are a few angstrom longer than those between the TM helices of the α-subunit. Thus, the subunits γ and β are less closely packed in the TM domain than the α-subunit helices in the 2-D crystals. However, these small distances largely depend on how the homology model is docked to the 3-D map. In addition, the presence of lipid molecules may influence the distances. In the 2-D crystals, Na,K-ATPase forms ribbons and the γ-subunit is located between two α-subunits, resulting also in proximity to M3 of an adjacent α-subunit. M3 is also suggested to be a potential interaction site between SERCA and pentameric phospholamban in 2-D cocrystals (Stokes et al., 2006).

In summary, we have determined the structure of renal Na,K-ATPase by cryoelectron microscopy using information to 8.0 Å resolution in the membrane plane. The structure resembles the E2 conformation, and docking a homology model to the experimental map reveals the location of the β-subunit close to the α-subunit helices M8 and M10 and that of the γ-subunit near helices M9 and M2.

This work was supported by grants from the Swedish Research Council, the Danish Medical Research Council and the Water and Salt Research Center (established and supported by the Danish National Research Foundation, Grundforskningsfonden). P. P. acknowledges a fellowship from the Emil Aaltonen Foundation.

## References

Axelsen, K.B., Palmgren, M.G. 1998. Evolution of substrate specificities in the P-type ATPase superfamily. *J. Mol. Evol.* **46:**84–101

Cantley, L.C. Jr., Cantley, L.G., Josephson, L. 1978. A characterization of vanadate interactions with the (Na,K)-ATPase. *J. Biol. Chem.* **253:**7361–7368

CCP4. 1994. The CCP4 suite: Programs for protein crystallography. *Acta Crystallogr. D* **50:**760–763

Colonna, T.E., Huynh, L., Fambrough, D.M. 1997. Subunit interactions in the Na,K-ATPase explored with the yeast two-hybrid system. *J. Biol. Chem.* **272:**12366–12372

Crowther, R.A., Henderson, R., Smith, J.M. 1996. MRC image processing programs. *J. Struct. Biol.* **116:**9–16

Donnet, C., Arystarkhova, E., Sweadner, K.J. 2001. Thermal denaturation of the Na,K-ATPase provides evidence for α-α oligomeric interaction and γ subunit association with the C-terminal domain. *J. Biol. Chem.* **276:**7357–7365

Forbush, B. 3rd, Kaplan, J.H., Hoffman, J.F. 1978. Characterization of a new photoaffinity derivative of ouabain: Labeling of the large polypeptide and of a proteolipid component of the Na,K-ATPase. *Biochemistry* **17:**3667–3676

Franzin, C.M., Choi, J., Zhai, D., Reed, J.C., Marassi, F.M. 2004. Structural studies of apoptosis and ion transport regulatory proteins in membranes. *Magn. Reson. Chem.* **42:**172–179

Füzesi, M., Gottschalk, K.-E., Lindzen, M., Shainskaya, A., Küster, B., Garty, H., Karlish, S.J.D. 2005. Covalent cross-links between the γ subunit (FXYD2) and α and β subunits of Na,K-ATPase. *J. Biol. Chem.* **280:**18291–18301

Geering, K. 2001. The functional role of β subunits in oligomeric P-Type ATPases. *J. Bioenerg. Biomembr.* **33:**425–438

Håkansson, K.O. 2003. The crystallographic structure of Na,K-ATPase N-domain at 2.6 Å resolution. *J. Mol. Biol.* **332:**1175–1182

Hasler, U., Crambert, G., Horisberger, J.-D., Geering, K. 2001. Structural and functional features of the transmembrane domain of the Na,K-ATPase β subunit revealed by tryptophan scanning. *J. Biol. Chem.* **276:**16356–16364

Hebert, H., Purhonen, P., Vorum, H., Thomsen, K., Maunsbach, A.B. 2001. Three-dimensional structure of renal Na,K-ATPase from cryo-electron microscopy of two-dimensional crystals. *J. Mol. Biol.* **314:**479–494

Hilge, M., Siegal, G., Vuister, G.W., Güntert, P., Gloor, S.M., Abrahams, J.P. 2003. ATP-induced conformational changes of the nucleotide-binding domain of Na,K-ATPase. *Nat. Struct. Biol.* **6:**468–474

Ivanov, A.V., Modyanov, N.N., Askari, A. 2002. Role of the self-association of β subunits in the oligomeric structure of $Na^+/K^+$-ATPase. *Biochem. J.* **364:**293–299

Ivanov, A., Zhao, H., Modyanov, N.N. 2000. Packing of the transmembrane helices of Na,K-ATPase: Direct contact between β-subunit and H8 segment of a α-subunit revealed by oxidative cross-linking. *Biochemistry* **39:**9778–9785

Jensen, A.-M.L., Sørensen, T.L.-M., Olesen, C., Møller, J.V., Nissen, P. 2006. Modulatory and catalytic modes of ATP binding by the calcium pump. *EMBO J.* **25:**2305–2314

Jones, T.A., Zou, J.Y., Cowan, S.W., Kjeldgaard, M. 1991. Improved methods for building protein models in electron density maps and the location of errors in these models. *Acta Crystallogr. A* **47:**110–119

Jørgensen, P.L. 1988. Purification of $Na^+,K^+$-ATPase: Enzyme sources, preparative problems and preparation from mammalian kidney. *Methods Enzymol.* **156:**29–43

Jørgensen, P.L., Håkansson, K.O., Karlish, S.J.D. 2003. Structure and mechanism of Na,K-ATPase: Functional sites and their interactions. *Annu. Rev. Physiol.* **65:**817–849

Keenan, S.M., DeLisle, R.K., Welsh, W.J., Paula, S., Ball, W.J. Jr 2005. Elucidation of the $Na^+,K^+$-ATPase digitalis binding site. *J. Mol. Graph. Model.* **23:**465–475

Kühlbrandt, W. 2004. Biology, structure and mechanism of P-type ATPases. *Nat. Rev. Mol. Cell. Biol.* **5:**282–295

Kunji, E.R.S., von Gronau, S., Oesterhelt, D., Henderson, R. 2000. The three-dimensional structure of halorhodopsin to 5 Å by electron crystallography: A new unbending procedure for two-dimensional crystals by using a global reference structure. *Proc. Natl. Acad. Sci. USA* **97:**4637–4642

Li, C., Grosdidier, A., Crambert, G., Horisberger, J.-D., Michielin, O., Geering, K. 2004. Structural and functional interaction sites between Na,K-ATPase and FXYD proteins. *J. Biol. Chem.* **279:**38895–38902

Lubarski, I., Pihakaski-Maunsbach, K., Karlish, S.J.D., Maunsbach, A.B., Garty, H. 2005. Interaction with the Na,K-ATPase and tissue distribution of FXYD5 (related to ion channel). *J. Biol. Chem.* **280:**33717–33724

Obara, K., Miyashita, N., Xu, C., Toyoshima, I., Sugita, Y., Inesi, G., Toyoshima, C. 2005. Structural role of countertransport revealed in $Ca^{2+}$ pump crystal structure in the absence of $Ca^{2+}$. *Proc. Natl. Acad. Sci. USA* **102:**14489–14496

Ogawa, H., Toyoshima, C. 2002. Homology modeling of the cation binding sites of $Na^+K^+$-ATPase. *Proc. Natl. Acad. Sci. USA* **99:**15977–15982

Olesen, C., Sørensen, T.L.-M., Nielsen, R.C., Møller, J.V., Nissen, P. 2004. Dephosphorylation of the calcium pump coupled to counterion occlusion. *Science* **306:**2251–2255

Or, E., Goldshleger, R., Karlish, S.J.D. 1999. Characterization of disulfide cross-links between fragments of proteolyzed Na,K-ATPase. *J. Biol. Chem.* **274:**2802–2809

Pettersen, E.F., Goddard, T.D., Huang, C.C., Couch, G.S., Greenblatt, D.M., Meng, E.C., Ferrin, T.E. 2004. UCSF chimera - a visualization system for exploratory research and analysis. *J. Comput. Chem.* **25:**1605–1612

Pu, H.X., Scanzano, R., Blostein, R. 2002. Distinct regulatory effects of the Na,K-ATPase γ subunit. *J. Biol. Chem.* **277:**20270–20276

Rice, W.J., Young, H.S., Martin, D.W., Sachs, J.R., Stokes, D.L. 2001. Structure of $Na^+,K^+$-ATPase at 11-Å resolution: Comparison with $Ca^{2+}$-ATPase in $E_1$ and $E_2$ states. *Biophys. J.* **80:**2187–2197

Šali, A., Blundell, T.L. 1993. Comparative protein modelling by satisfaction of spatial restraints. *J. Mol. Biol.* **234:**779–815

Sørensen, T.L.-M., Møller, J.V., Nissen, P. 2004. Phosphoryl transfer and calcium ion occlusion in the calcium pump. *Science* **304:**1672–1675

Stokes, D.L., Pomfret, A.J., Rice, W.J., Glaves, J.P., Young, H.S. 2006. Interactions between $Ca^{2+}$-ATPase and the pentameric form of phospholamban in two-dimensional co-crystals. *Biophys. J.* **90:**4213–4223

Sweadner, K.J., Donnet, C. 2001. Structural similarities of Na,K-ATPase and SERCA, the $Ca^{2+}$-ATPase of the sarcoplasmic reticulum. *Biochem. J.* **356:**685–704

Sweadner, K.J., Rael, E. 2000. The *FXYD* gene family of small ion transport regulators or channels: cDNA sequence, protein signature sequence, and expression. *Genomics* **68:**41–56

Therien, A.G., Pu, H.X., Karlish, S.J.D., Blostein, R. 2001. Molecular and functional studies of the gamma subunit of the sodium pump. *J. Bioenerg. Biomembr.* **33:**407–414

Toyoshima, C., Asahi, M., Sugita, Y., Khanna, R., Tsuda, T., MacLennan, D.H. 2003. Modeling of the inhibitory interaction of phospholamban with the $Ca^{2+}$ATPase. *Proc. Natl. Acad. Sci. USA* **100:**467–472

Toyoshima, C., Mizutani, T. 2004. Crystal structure of the calcium pump with a bound ATP analogue. *Nature* **430:**529–535

Toyoshima, C., Nakasako, M., Nomura, H., Ogawa, H. 2000. Crystal structure of the calcium pump of the sarcoplasmic reticulum at 2.6 Å resolution. *Nature* **405:**647–655

Toyoshima, C., Nomura, H. 2002. Structural changes in the calcium pump accompanying the dissociation of calcium. *Nature* **418:**605–611

Toyoshima, C., Nomura, H., Tsuda, T. 2004. Lumenal gating mechanism revealed in calcium pump crystal structures with phosphate analogues. *Nature* **432:**361–368

Wang, S.-G., Farley, R.A. 1998. Valine 904, tyrosine 898 and cysteine 908 in Na,K-ATPase α subunits are important for assembly with β subunits. *J. Biol. Chem.* **273:**29400–29405

Wriggers, W., Milligan, R.A., McCammon, A. 1999. Situs: A package for docking crystal structures into low-resolution maps from electron microscopy. *J. Struct. Biol.* **125:**185–195

Zouzoulas, A., Blostein, R. 2006. Regions of the catalytic α subunit of Na,K-ATPase important for functional interactions with FXYD 2. *J. Biol. Chem.* **281:**8539–8544